NANOCOMPOSITE BASED ON HYDROXYAPATITE AND SILVER WITH ANTIBACTERIAL ACTIVITY

Aurora MOCANU[a], Diana Alexandra FLOREA[a], Gheorghe TOMOAIA[b,c], Lucian-Cristian POP[a,*], Ancuta DANISTEAN[a], Sorin RAPUNTEAN[d], Ossi HOROVITZ[a] and Maria TOMOAIA-COTISEL[a,c,*]

ABSTRACT. A nanocomposite made from hydroxyapatite (HAP) and silver nanoparticles (AgNPs), namely HAP-4.5 wt% AgNPs, is reported. HAP was prepared using a wet precipitation technique, and AgNPs were made by reducing silver nitrate with glucose in basic medium. HAP, AgNPs and HAP-4.5 wt% AgNPs composite were characterized by X-ray diffraction (XRD), SEM - energy dispersive X-ray spectroscopy (EDS) and different imagistic methods: TEM and AFM. The antibacterial effect of the HAP-4.5 wt% AgNPs nanocomposite was tested using diffusion technique in nutritive agar on two pathogenic species, one Gram-negative (*Salmonella typhimurium*) and one Gram-positive (*Bacillus cereus*) and promising results were obtained. This hydroxyapatite-silver nanocomposite can be employed as a potential antimicrobial coating for dental and orthopedic implants, or they can be utilized such as bone cements in clinical procedures.

Keywords: hydroxyapatite, silver nanoparticles, nanocomposite, antibacterial activity, pathogens

a *Babes-Bolyai University of Cluj-Napoca, Faculty of Chemistry and Chemical Engineering, Research Centre of Physical Chemistry, 11 Arany Janos Str., Cluj-Napoca, 400084, Romania*
b *Iuliu Hatieganu University of Medicine and Pharmacy, Orthopedics and Traumatology, 47 Gen. Traian Mosoiu Str., Cluj-Napoca, 400132, Romania*
c *Academy of Romanian Scientists, 3 Ilfov Str., RO-400132, Bucharest, Romania*
d *University of Agricultural Sciences and Veterinary Medicine of Cluj-Napoca, 3-5 Manastur Str., Cluj-Napoca, 400372, Romania*
* *Corresponding authors: Lucian-Cristian Pop lucian.pop@ubbcluj.ro; Maria Tomoaia-Cotisel maria.tomoaia@ubbcluj.ro*

AURORA MOCANU, DIANA ALEXANDRA FLOREA, GHEORGHE TOMOAIA, LUCIAN-CRISTIAN POP, ANCUTA DANISTEAN, SORIN RAPUNTEAN, OSSI HOROVITZ, MARIA TOMOAIA-COTISEL

INTRODUCTION

The finding of the earliest antibiotic, penicillin, by Alexander Fleming in 1928 revolutionized medicine and saved countless lives by providing a way to effectively treat bacterial infections [1]. Since then, almost a century has passed and bacteria, due to misuse, have evolved resistance to antibiotics through mutations that led to drug-resistant bacteria, which are a foremost threat to public health [2, 3]. Although some metal ions, like Ag, Cu, Zn, and Au, have long been acknowledged to have antibacterial characteristics, they were "forgotten" during the successful era of antibiotics. Silver nanoparticles, known for their antimicrobial properties for centuries, have been proposed as a potential solution to combat drug-resistant bacteria. Due to their insignificant dimension and huge surface area, AgNPs can interfere with bacterial cell walls by disrupting the cellular processes leading to bacterial death [4, 5].

Silver nanoparticles (AgNPs) produced *via* a variety of techniques, including chemical, physical, photochemical and biological, were found to have an antibacterial effect [6-14]. AgNPs produced in various formulations, with diverse shapes and sizes, show variable antimicrobial activity, while the mechanism of antimicrobial effect of Ag ions and AgNPs, as well as their toxicity on tissues, are not fully elucidated [15-20]. The antibacterial effect of AgNPs was associated with their shape, with triangular particles presenting a more intense effect compared to spherical ones [21-23]. Compared to other metals, silver has a high toxicity against microorganisms and a much lower toxicity against mammalian cells [24-26].

The human body contains nanosize hydroxyapatite (HAP), an inorganic mineral ($Ca_{10}(PO_4)_6(OH)_2$) having a Ca to P mole ratio of 5/3 (cca 1.67). It is found within the bone as a bioactive ceramic that covers about 70% of bone weight and in teeth that covers up to 80% of dentin and enamel.

Crystallographic and chemical studies revealed that synthetic HAP is comparable to natural HAP. Due to this fact, synthetic HAP is also considered a great option for bone or dental reconstruction because it is osteoconductive, stable at physiological pH, biocompatible, and readily adsorbed with bioorganic substances (proteins, amino acids, etc.).

As a support and carrier for AgNPs, both pure hydroxyapatite (HAP) and doped HAP with various cations or anions, were also used as nanomaterials of choice [27-35]. As an alternative, HAP doped with silver ions was also used as antimicrobial material [36-41]. HAP-AgNPs composites with organic polymers were also used [42-47], to ensure a retarded silver ion release.

Here we intended to synthesize a hydroxyapatite with a low degree of crystallization and high porosity, able to assure a good adsorption and release of silver nanoparticles. For the synthesis of HAP with the desired characteristics, we use a chemical precipitation method developed by us [39, 48-55]. By reducing silver nitrate with glucose, silver nanoparticles are obtained [49]. In addition, some microbiological tests were performed having in mind to assess the antimicrobial properties of the newly synthetized nanocomposite.

RESULTS AND DISCUSSION

Characterization of AgNPs

The UV-Vis spectrum of the dispersion containing AgNPs presents the specific SPR absorption band of Ag, with the maximum at 405 nm (Fig. 1A). The spectrum did not change in time for 1 year, thus evidencing the high stability of the AgNPs dispersion.

TEM image for AgNPs is depicted in Fig. 1. The mean diameter of the AgNPs was found to be 13.0 ± 2 nm.

A   B
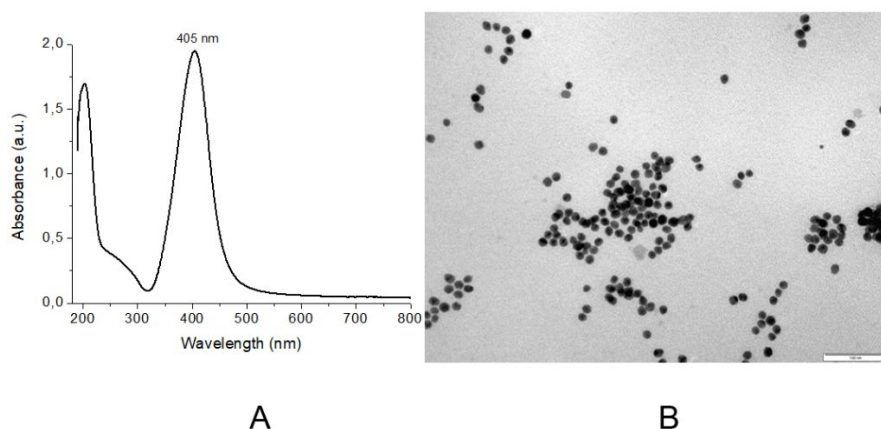
Fig. 1. UV-Vis spectrum for AgNPs aqueous dispersion (A) and TEM image for AgNPs (B); the scale bar is 100 nm. The average diameter of AgNPs is around 13 nm. The zeta potential value for AgNPs is negative, -39 mV, ensuring a high electrostatic stability of the AgNPs dispersion.

AURORA MOCANU, DIANA ALEXANDRA FLOREA, GHEORGHE TOMOAIA, LUCIAN-CRISTIAN POP, ANCUTA DANISTEAN, SORIN RAPUNTEAN, OSSI HOROVITZ, MARIA TOMOAIA-COTISEL

Characterization of HAP-4.5 wt% Ag composite

The samples do not differ significantly from each other. The HAP nanoparticles present a rather low degree of crystallinity, as wanted by the synthesis. The presence of crystalline silver is evidenced in Fig. 2 for HAP-4.5 wt% Ag where the lines for silver from PDF 89-3722 are shown. Their position is in good agreement with that found for nanosilver particles [56] for the (111), (200), (220), (311) and (222) planes of Ag, corresponding to the peaks at 2θ values of 38.32, 44.50, 64.61, 77.54 and 81.68° respectively. In Figure 2, the most intense diffraction of silver [(111) plane] in HAP-4.5 wt% Ag appears distinctly, while the other Ag diffraction lines are partially superposed on the diffraction peaks of HAP.
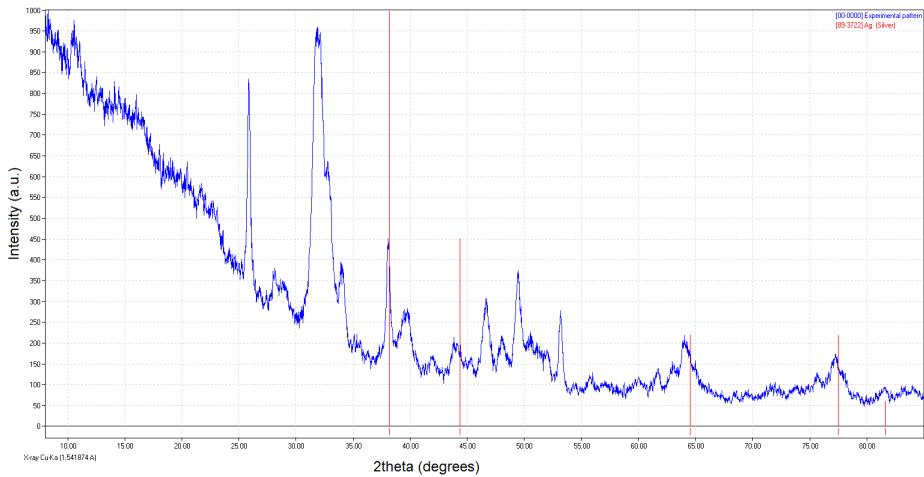
Fig. 2. XRD pattern for HAP-4.5 wt% Ag compared with PDF 89-3722 for Ag (vertical red lines)

The typical crystallite dimensions and the crystallinity amount of the samples are given in Table 1.

Table 1. Average crystallite size and crystallinity degree of HAP and HAP-4.5 wt% Ag composite, from XRD data; NPs average diameter of composite from AFM investigation

Sample	HAP [57]	HAP-4.5 wt% Ag	HAP-4.5 wt% Ag (AFM Fig. 4)
Crystallites size (nm)	47.6	45.3	-
Crystallinity (%)	36	37	-
Average diameter of NPs (nm)	-	-	54 ± 8nm

The average diameter of HAP-4.5 wt% AgNPs is 54 ± 8nm, as obtained from AFM measurements (Fig. 4), which is somewhat higher than about 45 nm obtained from XRD measurements (Fig. 2) and to about 48 nm found for pure HAP. Thus, the average diameter of HAP-4.5 wt% AgNPs composite is only slightly increased by mixing HAP NPs with AgNPs for this composition.

In the SEM-EDS (EDX) spectrum, fig. 3, the presence of Ag is revealed, along with the elements which enter in the composition of HAP (Ca, P, O), as shown in Fig. 3B. Cu and C also appear in the spectrum, since the grids on which the particles were adsorbed are made from carbon coated copper. The uniform distribution of AgNPs in the sample is also evident in Fig. 3A and Fig. 4A.
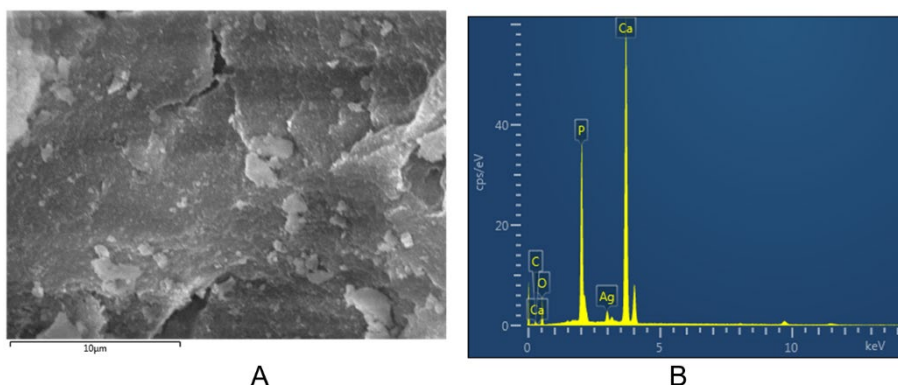
Fig. 3. SEM image (A) and EDX spectrum (B) for HAP-4.5 wt% AgNPs.

AFM images for the HAP-4.5% Ag nanocomposite, on sample obtained by adsorption on glass plate, are presented in Fig. 4. As shown in AFM images (A, B and C) and from the cross-section profile (D), the average particle size is 54 nm ± 8nm in this nanocomposite.
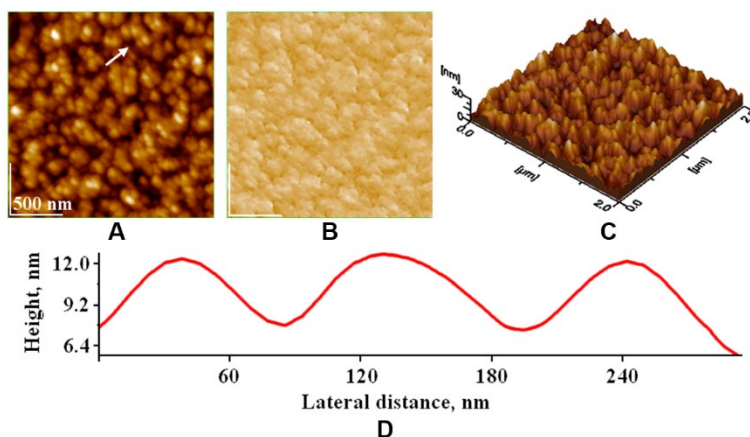
Fig. 4. AFM images of HAP-4.5 wt% AgNPs adsorbed on glass plate**:** A) topographic image, B) amplitude image, C) 3D image, and D) profile on the white arrow in panel (A). Scanned area 2 µm x 2 µm. Maximum height 30 nm, surface roughness evaluated as root mean square, Rrms = 4.8 nm. Average particle diameter is determined from many profiles (at least 10) as 54 nm ± 8nm.

Zeta potential measurements for HAP dispersions gave a slightly negative value: -6.5 mV.

Antimicrobial effect

After the incubation period, the plates were examined and the diameters of the inhibition zones (in mm) were determined. Values of 13 mm was found for *Salmonella typhimurium (*ATCC 14028) and 12 mm for *Bacillus cereus* (ATCC 14579).

The results evidence a clear inhibitory effect of HAP-Ag composite on the verified bacterial strains, whereas no inhibition zone is detected for the witness sample (pure HAP). The silver content in a well corresponding to the HAP-4.5 wt% Ag composite is 32 µg.

When comparing the different bacterial strains, we find only small differences. The most sensible appears to be *Salmonella typhimurium* followed by *Bacillus cereus*.

CONCLUSIONS

In conclusion, a straightforward technique for synthesizing HAP-AgNPs with a silver content of 4.5 wt% was effectively developed. Using the XRD, SEM-EDS, TEM, and AFM, the morphological and compositional characteristics of the as-prepared nanocomposite were verified. TEM, SEM, and AFM images showed the dimension and form of HAP particles, both with and without AgNPs, and XRD and EDS measurements confirmed the presence of silver.

Equally Gram-negative and Gram-positive isolates were effectively killed by the HAP-4.5wt%AgNPs that was under investigation. These findings imply that our composite could be regarded as antibacterial materials and that they could be utilized in dentistry and orthopedic implants.

EXPERIMENTAL SECTION

Materials and methods

Materials: As precursors were used: calcium nitrate tetrahydrate, $Ca(NO_3)_2 \cdot 4H_2O$ (p.a., Poch S.A., Poland), alongside with diammonium hydrogen phosphate, $(NH_4)_2HPO_4$ (p.a., Nordic Invest, Romania); glucose (10% solution, Hemofarm, Braun Pharmaceuticals S.A., Timisoara, Romania), silver nitrate, $AgNO_3$ (analytical purity, Merck, Germany) and NaOH (10% solution, Sigma-Aldrich, Germany).

Preparation of HAP-Ag samples

Synthesis of low crystallinity hydroxyapatite (HAP). Low crystallinity nano hydroxyapatite (HAP) was synthetized *via* a wet chemical process, with $Ca(NO_3)_2 \cdot 4H_2O$ and $(NH_4)_2HPO_4$ as starting materials [57]. A 250 mM $Ca(NO_3)_2$ solution was obtained in bidistilled water with added 25% ammonia solution (pH 8.5), and another 150 mM $(NH_4)_2HPO_4$ solution in bidistilled water, containing ammonia solution (pH 11). These solutions were quickly mixed at 0 °C. The dispersion, as obtained in the mother liquor was allowed to mature 10 h at 22 °C (under intermittent stirring), then filtered and rinsed with bidistilled water until no NO_3^- is found. For further characterization, a portion of the watery precipitate was desiccated by lyophilization. The wet precipitate separated by filtration (containing 80% water) was used as scaffold for AgNPs.

13

Preparation of AgNPs. A method using the reduction of Ag^+ ions by glucose, in a basic solution was used. This implied the reduction of silver nitrate, $AgNO_3$ (analytical purity, Merck, Germany) in a very diluted aqueous solution (final concentration $0.25 \cdot 10^{-3}$ M, silver content 27 mg/L) with glucose (10 % aqueous solution), the glucose being in large excess: 0.5 ml glucose solution / 1 mg Ag (molar ratio glucose/Ag = 30) in alkaline medium (pH cca. 12, obtained with the help of a 10% NaOH solution) at room temperature (22 °C). Silver nanoparticles were dispersed, giving off a light yellowish-brown tint.

Preparation of HAP-4.5% Ag composite. The AgNPs aqueous dispersion is added under continuous magnetic stirring to the wet HAP precipitate in the ratio needed for an Ag content in the HAP-Ag composite of 4.5 %. (For instance, to 1 g wet HAP precipitate (80% water) 350 mL AgNPs dispersion were added). The stirring continues for 2h, and the mixture is let to stay for 24 h at 22 °C. Then the HAP-Ag precipitate is filtered and desiccated at ambient temperature.

Characterization methods

X-ray diffraction (XRD) patterns have been produced employing a DRON-3 diffractometer (Bragg–Brentano geometry) fitted with an X-ray tube with copper K_α radiation, $\lambda = 1.541874$ Å, in the domain between 5° and 85° 2θ.

Comparing the peaks of the diffraction images with PDF allowed the identification of phases [58-63]. The peak locations of the diffraction patterns were compared to PDF (Powder Diffraction File) 74-0566 belonging to stoichiometric HAP and PDF 89-3722 for silver to determine the phases.

UV-Vis absorption spectra were measured between 190 and 900 nm by means of a Jasco UV/Vis V-650 spectrophotometer and 1 cm quartz cuvettes, at ambient temperature. HAP water dispersions required for TEM and AFM imaging were obtained by ultra-sonification (Sonics Vibra-Cell, VCX 750), for 5 min, at room temperature.

TEM images acquired with TEM, JEOL – JEM 1010 equipment were captured with JEOL typical software. *SEM* images were obtained with a scanning transmission electron microscope, STEM Hitachi HD-2700. Also, energy-dispersive *X-ray* spectrum (*EDS* or *EDX*) of the distribution and relative proportion of elements was obtained over the scanned areas.

The AFM JEOL 4210 apparatus was run in tapping mode [64-69] using conventional silicon nitride-tipped cantilevers (resonant frequency: 200–300 kHz; spring constant: 17.5 N/m). The particles were adsorbed from their ultrapure water dispersion for 10 s on glass plates. On the same adsorbed film, various regions ranging in size from 10 μm x 10 μm to 0.5 μm x 0.5 μm were scanned. The various obtained images have been managed by usual AFM JEOL procedures.

On aqueous dispersions of the AgNPs, zeta potential readings were made with a Malvern Zetasizer Nano-ZS90 apparatus.

Antibacterial assays

The bacterial strains tested were: *Bacillus cereus* ATCC 14579 and *Salmonella typhimurium* ATCC 14028. The microbial strains were inseminated in glucose medium (nutrient broth and nutrient agar) (TM Media, Titan Biotech, India), and incubated in a thermostat (37 °C), under aerobic conditions, for a period of 18-24 h. The microbial strains have been verified by bacteriological examination. The tested microbial strains are checked every time by a bacteriological test, to appreciate the culture characteristics, both in liquid and solid medium, as well as the morphological characters, on smears stained by Gram's method. This is done in order to have a pure culture and to use a young culture of 24 h.

The inhibiting effect is assessed by the antibiogram technique of diffusion in nutritive agar gel, adapted for testing products treated as suspensions. For this, nutritive agar, supplemented with glucose and NaCl, was liquefied by warming in a water bath and transferred to 90 mm diameter Petri dishes in a volume of 25 ml, giving a 3 mm thick even layer of 3 mm thick. Flood inoculation was applied, using a 1 ml suspension made from the tested strain at density 0.5, according to McFarland standards. The uniform dispersion on the entire surface is done using a Drigalski spate. After drying of the agar surface (20 minutes in the thermostat with half-open lid), the wells (diameter 0.6 cm) are cut out in the agar gel in a circular shape. Amounts of 0.2 g of HAP-4.5 wt% Ag sample and pure HAP (as a witness) were dispersed in 2 ml of water and then an amounts of 35 µl were distributed in the wells. For 18-24 hours, the dishes were incubated at 37 °C in a thermostat. The plates were read in order to identify the existence or non-existence of culture growth around the wells. The span of the inhibition zone (expressed in millimetres) was determined if an inhibitory effect was seen. The dishes were monitored for an additional 5 days to spot any variations over time.

REFERENCES

1. R. Gaynes, *Emerg. Infect. Dis.,* **2017**, *23*(*5*), 849-853.
2. R. Urban-Chmiel; A. Marek; D. Stępień-Pyśniak; K. Wieczorek; M. Dec; A. Nowaczek; J. Osek; *Antibiotics (Basel, Switzerland),* **2022**, *11*(*8*), 1079.
3. D.G.J. Larsson; C.-F. Flach; *Nat. Rev. Microbiol.,* **2022**, *20*(*5*), 257-269.

4. E. Urnukhsaikhan; B.-E Bold; A. Gunbileg; N. Sukhbaatar; T. Mishig-Ochir; *Sci. Rep.,* **2021**, *11*(*1*), 21047.
5. S.A. Ahmad; S.S. Das; A. Khatoon; M.T. Ansari; M. Afzal; M.S. Hasnain; A.K. Nayak; *Mater. Sci. Technol.,* **2020**, *3*, 756-769.
6. S. Rajeshkumar; C. Malarkodi; M.Vanaja; G. Annadurai; *J. Mol. Struct.,* **2016**, *1116,* 165-173.
7. M. Bhat; B. Chakraborty; R.S. Kumar; A.I. Almansou; N. Arumugam; D.Kotresha; S. Pallavi, S. Dhanyakumara; K. Shashiraj; S. Nayaka; *J. King Saud Univ. Sci.*, **2021**, *33*, 101296.
8. M.M.N. El-Dein; Z.A.M. Baka; M.I. Abou-Dobara; A.K. El-Sayed; M.M. El-Zahed; *J. Microbiol. Biotechnol. Food Sci.*, **2021**, *10*, 648–656.
9. J.S. Gabriel; V.A.M. Gonzaga; A.L. Poli; C.C. Schmitt; *Carbohydr. Polym.*, **2017**, *171*, 202-210.
10. G.A. Bhaduri; R. Little; R.B. Khomane; S.U. Lokhande; B.D. Kulkarni; B.G. Mendis; L. Šiller; *J. Photochem. Photobiol. A: Chemistry,* **2013**, *258*, 1-9.
11. M. Mohammadlou; Maghsoudi H; H. Jafarizadeh-Malmiri; *Int. Food. Res. J.*, **2016**, *23*(*2*), 446-463.
12. S. Kaviya; J. Santhanalakshmi; B. Viswanathan; J. Muthumary; K. Srinivasan; *Spectrochim. Acta A Mol. Biomol. Spectrosc.,* **2011**, *79*(*3*), 594-598.
13. N.G. Mlalila; H.S. Swai; A. Hilonga; D.M. Kadam; *Nanotechnol. Sci. Appl.,* **2017**, *10*, 1-9.
14. S. Ullah Khan; T.A. Saleh; A. Wahab; M.H. Ullah Khan; D. Khan; W. Ullah Khan; A. Rahim; S. Kamal; F. Ullah Khan; S. Fahad; *Int. J. Nanomed.*, **2018**, *13*, 733-762.
15. M. Zahoor; N. Nazir; M. Iftikhar; S. Naz; I. Zekker; J. Burlakovs; F. Uddin; A.W. Kamran; A. Kallistova; N. Pimenov; F.A. Khan; *Water,* **2021**, 1*3*(*16*), 2216.
16. P.R. More; S. Pandit; A. Filippis; G. Franci; I. Mijakovic; M. Galdiero; *Microorganisms*, **2023,**11(*2*), 369.
17. Y. Yang; X. Chen; N. Zhang; B. Sun; K. Wang; Y. Zhang; L. Zhu; *Water Research*, **2022**, *218*, 118452.
18. A. Luceri; R. Francese; D. Lembo; M. Ferraris; C. Balagna; *Microorganisms*, **2023**,11(*3*), 629.
19. T. Bruna; F. Maldonado-Bravo; P. Jara; N. Caro; *Int. J. Mol. Sci.*, **2021**, *22*(*13*), 7202.
20. H.A. Hemeg; *Int. J. Nanomed.*, **2017**, *12*, 8211-8225.
21. P. Sukdeb; Y.K. Tak; J.M. Song; *Appl. Environ. Microbiol.*, **2007**, *73*(*6*),1712-1720.
22. M.F. Anwar; D. Yadav; S. Jain; S. Kapoor; S. Rastogi; I. Arora; M. Samim; *Int. J. Nanomed.,* **2016**, *11*, 147-158.
23. J.Y. Cheon; S.J. Kim; Y.H. Rhee; O.H. Kwon, W.H. Park; *Int. J. Nanomed.,* **2019**, *14,* 2773-2780.
24. G. Zhao; S.E. Stevens; *Biometals*, **1998**, *11*, 27-32.
25. M. Ema, H. Okuda, M. Gamo, K. Honda; *Reprod. Toxicol.,* **2017**, *67*,149-164.
26. F.J. Osonga; A. Akgul; I. Yazgan; A. Akgul; G.B. Eshun; L. Sakhaee; O.A. Sadik; *Molecules,* **2020**, *25*(*11*), 2682.
27. P. Phatai; N. Prachumrak; S. Kamonwannasit; A. Kamcharoen; W. Roschat; S. Phewphong; C.M. Futalan; P. Khemthong; T. Butburee; S. Youngjan; J.C. Millare; O. Prasitnok; *Sustainability,* **2022**, *14*, 11756.

28. A. Nenen; M. Maureira; M. Neira; S.L. Orellana; C. Covarrubias; I. Moreno-Villoslada; *Ceram. Int.*, **2022**, *48*(*23*), A, 34750-34759.
29. V. Stanić; S. Dimitrijević; J. Antić-Stanković; M. Mitrić; B Jokić; I. B. Plećaš; S. Raičević; *Appl. Surf. Sci.*, **2010**, *256*(*20*), 6083-6089.
30. S. Kamonwannasit; C.M. Futalan; P. Khemthong; T. Butburee; A. Karaphun; P. Phatai; *J. Sol-Gel Sci. Technol.*, **2020**, *96,* 452-463.
31. T. Tithito; S. Sillapaprayoon; W. Pimtong; J. Thongbunchoo; N. Charoenphandhu; N. Krishnamra; A. Lert-Itthiporn; W. Maneeprakorn; W. Pon-On; *Nanomaterials (Basel)*, **2023**, *13*(*2*), 255.
32. S. Sprio; M. Dapporto; L. Preti; E. Mazzoni; M.R. Iaquinta; F. Martini; M. Tognon; N.M. Pugno; E. Revisto; L. Visai; A. Tampieri; *Front. Mater.*, **2020**, *7*, 224.
33. A. Z. Alshemary; A. E. Pazarceviren; T. Aysen; E. Zafer; *RSC Advances*, **2016**, *6*(*72*), 68058-68071.
34. P.N. Lim; L. Chang; E.S. Thian; *Nanomedicine*, **2015**, *11*(*6*) 1331-1344.
35. R. Ahmadi; S. Izanloo; *J. Mech. Behav. Biomed. Mater.*, **2022**, *126*, 105075.
36. F.A.C. Andrade; L.C. de Oliveira Vercik; F.J. Monteiro; E.C. da Silva Rigo; *Ceram. Int.*, **2016**, *42*(*2*), 2271-2280.
37. P.N. Silva-Holguín; S.Y. Reyes-López; *Dose-Response*, **2020**,*18*(*3*).
38. S. Jadalanagan; K. Deshmukh; S.R. Ramanan; M. Kowshik; *Appl. Nanosci.*, **2014**, *4*(*2*), 133-141.
39. A. Mocanu; G. Furtos; S. Rapuntean; O. Horovitz; C. Flore; C. Garbo; A. Danisteanu; G. Rapuntean; C. Prejemrean; M. Tomoaia-Cotisel; *Appl. Surf. Sci.*, **2014**, *298*, 225-235.
40. S. Elbasuney; G.S. El-Sayyad; S.M. Radwan; M. A. Correa-Duarte; *J. Inorg. Organomet. Polym.*, **2022**, *32*, 4559-4575.
41. S. L. Iconaru; D. Predoi; C.S. Ciobanu; M. Motelica-Heino; R. Guegan; C. Bleotu; *Coatings*, **2022**, *12*, 341.
42. L.F.B. Nogueira; M.A. Eufrásio Cruz; G.J. Aguilar; D.R. Tapia-Blácido; M.E. da Silva Ferreira; B.C. Maniglia; M. Bottini; P. Ciancaglini; A.P. Ramos; *Int. J. Mol. Sci.*, **2022**, *23*(*13*), 7277.
43. Y. Zhang; V.J. Reddy; S.Y. Wong; X. Li; B. Su; S. Ramakrishna; C.T. Lim; *Tissue Eng. Part A.*, **2010**, *16*(*6*), 1949-1960.
44. J. P. Monte; A. Fontes; S. Beate; S. Santos; G.A.L. Pereira; G. Pereira; *Mater. Lett.*, **2023**, *338*, 134027.
45. R. Choubey; R. Chouhan; A.K. Bajpai; J. Bajpai; S.K. Singh, *Int. J. Polym. Mater. Polym.*; **2021**, *70* (*11*), 782-796.
46. F. Liu; X. Wang; T. Chen; N. Zhang; Q. Wei; J. Tian; Y. Wang; C. Ma; Y. Lu, *J. Adv. Res.*; **2020**, *21*, 91-102.
47. R.K. Saini; L.P. Bagri; A.K. Bajpa; *Colloids Surf. B*, **2019**, *177*, 211-218.
48. C. Garbo; M. Sindilaru; A. Carlea; Gh. Tomoaia; V. Almasan; I. Petean; A. Mocanu; O. Horovitz; M. Tomoaia-Cotisel; *Part. Sci. Technol.*, **2017,** *35*(*1*), 29.
49. Gh. Tomoaia; A. Mocanu; I. Vida-Simiti; N. Jumate; L.-D. Bobos; O. Soritau; M. Tomoaia-Cotisel; *Mater. Sci. Eng. C*, **2014**, *37*(*1*), 37- 47.

50. D. Oltean-Dan; G.-B. Dogaru; M. Tomoaia-Cotisel; D. Apostu; A. Mester; H.-R.-C. Benea; M.-Gh. Paiusan; E.-M. Jianu; A. Mocanu; R. Balint; C.-O. Popa; C. Berce; G.-I. Bodizs; A.-M. Toader; Gh. Tomoaia; *Int. J. of Nanomed.*, **2019**, *14*, 5799-5816.

51. Gh. Tomoaia; O. Soritau; M. Tomoaia-Cotisel; L.-B. Pop; A. Mocanu; O. Horovitz; L.-D. Bobos; *Powder Technol.*, **2013**, *107*, 23899.

52. A. Mocanu; R.D. Pasca; Gh. Tomoaia; C. Garbo; P.T. Frangopol; O. Horovitz; M. Tomoaia-Cotisel; *Int. J. Nanomed.*, **2013**, *8*, 3867-3874.

53. D. Oltean-Dan; G.-B. Dogaru; E.-M. Jianu; S. Riga; M. Tomoaia-Cotisel; A. Mocanu; L. Barbu-Tudoran; Gh. Tomoaia; *Micromachines*; **2021**, *12*, 1352.

54. A. Mocanu; O. Cadar; P.T. Frangopol; I. Petean; Gh. Tomoaia, G.-A. Paltinean; Cs.P. Racz, O. Horovitz; M. Tomoaia-Cotisel; *R. Soc. Open. Sci.*, **2021**, *8*(*1*), 201785.

55. A. Avram; T. Frentiu; O. Horovitz; A. Mocanu; F. Goga; M. Tomoaia-Cotisel; *STUDIA UBB Chemia*, **2017**, *62*(*4*), 93-104.

56. T. Theivasanthi; M. Alagar; *Nano Biomed. Eng.*, **2012**, *4*, 58-65.

57. A. Mocanu; R. Balint; C. Garbo; I. Timis; I. Petean; O. Horovitz; M. Tomoaia-Cotisel, *STUDIA UBB Chemia*, **2017**, 62, *2*(*1*), 95-103.

58. Zs. Pap; E. Karácsonyi; L. Baia; L.-C. Pop; V. Danciu; K. Hernádi; K. Mogyorósi; A. Dombi; *Phys. Status Solidi B*, **2012**, *12*, 2592-2595.

59. E. Karácsonyi; L. Baia; A. Dombi; V. Danciu; K. Mogyorósi; L.-C. Pop; G. Kovács; V. Coșoveanu; A. Vulpoi; S. Simon; Zs. Pap; *Catal. Today*, **2013**, *208*, 19-27.

60. S. Sfaelou; L.-C. Pop; O. Monfort; V. Dracopoulos; P. Lianos; *Int. J. Hydrog. Energy.*, **2016**, *41*, 5902–5907.

61. M. Popa; L.C. Pop; G. Schmerber; C. Bouillet; O. Ersen; *Appl. Surf. Sci.*, **2021**, *562*, 150159.

62. A.I. Cadiş; L.E. Mureșan; I. Perhaița; L. C. Pop; K. Saszet; L. Barbu-Tudoran; G. Borodi; *J. Nanopart. Res.*, **2022**, *24*, 74.

63. E.-Z.Kedves; C. Fodor; Á. Fazekas; I. Székely; Á. Szamosvölgyi; A. Sápi; Z. Kónya; L.C. Pop; L. Baia; Z. Pap; *Appl. Surf. Sci.*, **2023**, *624*,156914.

64. U.V. Zdrenghea; Gh. Tomoaia; D.-V. Pop-Toader; A. Mocanu; O. Horovitz; M. Tomoaia-Cotisel; *Comb. Chem. High Throughput Screen.*, **2011**, *14*(*4*), 237-247.

65. L.Z. Racz; G.-A. Paltinean; I. Petean; Gh. Tomoaia; L. C. Pop; G. Arghir; E. Levei; A. Mocanu; Cs.-P. Racz; M. Tomoaia-Cotisel; *STUDIA UBB Chemia*, **2022**, *67*(*3*), 61-74.

66. Cs.-P. Racz; L.Z. Racz; C.G. Floare; Gh. Tomoaia; O. Horovitz; S. Riga; I. Kacso; Gh. Borodi; M. Sarkozi; A. Mocanu; C. Roman; M. Tomoaia-Cotisel; *Food. Hydrocoll.*, **2023**, *139*, 1088547.

67. M. Tomoaia-Cotisel; A. Tomoaia-Cotisel; T. Yupsanis; Gh. Tomoaia; I. Balea; A. Mocanu; Cs-P. Racz; *Rev. Roum. Chim.*, **2006**, *51*(*12*), 1181-1185.

68. O. Horovitz; Gh. Tomoaia; A. Mocanu; T. Yupsanis; M. Tomoaia-Cotisel; *Gold Bull.*, **2007**, *40*(*4*), 295-304.

69. O. Monfort; L.-C. Pop; S. Sfaelou; T. Plecenik; T. Roch; V. Dracopoulos; E. Stathatos; G. Plesch; P. Lianos; *Chem. Eng. J.*, **2016**, *286*, 91-97.